AD-A098 824 DEPARTMENT OF COMMERCE WASHINGTON DC F/G 5/1
THERMODYNAMICS OF HIGH TEMPERATURE MATERIALS.(U)
SEP 80 D A DITMARS, S ABRAMOWITZ, A MILLER AFOSR-ISSA-80-00007
UNCLASSIFIED AFOSR-TR-81-0443 NL

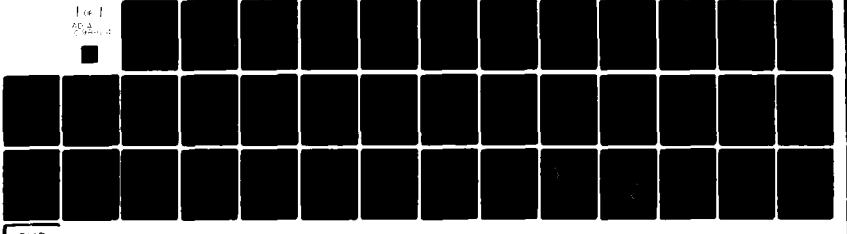

END
DATE FILMED
6-81
DTIC

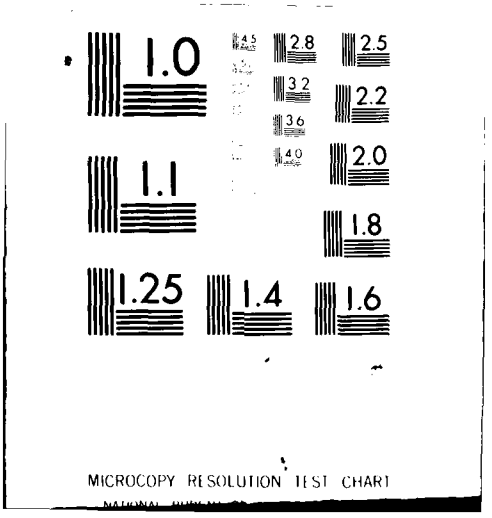
1.0
2.8
2.5
3.2
2.2
3.6
4.0
2.0
1.1
1.8
1.25
1.4
1.6
MICROCOPY RESOLUTION TEST CHART

UNCLASSIFIED

SECURITY CLASSIFICATION OF THIS PAGE (When Data Entered)

REPORT DOCUMENTATION PAGE	READ INSTRUCTIONS BEFORE COMPLETING FORM
1. REPORT NUMBER: AFOSR-TR-81-0443	2. GOVT ACCESSION NO.: AD A098824
3. RECIPIENT'S CATALOG NUMBER: 12 36	
4. TITLE (and Subtitle): THERMODYNAMICS OF HIGH TEMPERATURE MATERIALS	5. TYPE OF REPORT & PERIOD COVERED: Interim - Annual
	6. PERFORMING ORG. REPORT NUMBER
7. AUTHOR(s): D. A. Ditmars S. Abramowitz A. Miller A. Cezairliyan M.S. Morse	8. CONTRACT OR GRANT NUMBER(s): AFOSR-ISSA-80-00007
9. PERFORMING ORGANIZATION NAME AND ADDRESS: United States Department of Commerce, National Bureau of Standards, Washington, D.C. 20234	10. PROGRAM ELEMENT, PROJECT, TASK AREA & WORK UNIT NUMBERS: 2306 A2, 61102F, A2
11. CONTROLLING OFFICE NAME AND ADDRESS: Air Force Office of Scientific Research, Bolling AFB, Bldg. 410, Washington, D.C. 20332	12. REPORT DATE: 11 SEP 80
	13. NUMBER OF PAGES: 33
14. MONITORING AGENCY NAME & ADDRESS (if different from Controlling Office): Annual rept. 1 Oct 79 - 30 Sep 80	15. SECURITY CLASS. (of this report): UNCLASSIFIED
	15a. DECLASSIFICATION/DOWNGRADING SCHEDULE

16. DISTRIBUTION STATEMENT (of this Report)

Approved for public release; distribution unlimited.

17. DISTRIBUTION STATEMENT (of the abstract entered in Block 20, if different from Report)

18. SUPPLEMENTARY NOTES

19. KEY WORDS (Continue on reverse side if necessary and identify by block number)

20. ABSTRACT (Continue on reverse side if necessary and identify by block number)

Heat capacity and electrical resistivity of a carbon--carbon composite has been measured in the range of 1500 to 3000 K. The melting point of palladium has been measured. Apparatuses for the measurement of thermal expansion and thermal diffusitivity are described. The enthalpy of pure silicon carbide has been measured in the range of 273 to 1200 K. A discussion of the experiments leading to the electronic ground state of FeO is provided. The vibrational spectrum of Boron trimethyl is provided with the thermodynamic implications.

DD FORM 1 JAN 73 1473 EDITION OF 1 NOV 65 IS OBSOLETE

UNCLASSIFIED

SECURITY CLASSIFICATION OF THIS PAGE (When Data Entered)

THERMODYNAMICS OF HIGH TEMPERATURE MATERIALS

Annual Report for the Period of
1 October 1979 - 30 September 1980

AIR FORCE OFFICE OF SCIENTIFIC RESEARCH
AFOSR-ISSA-80-00007

Abstract

Heat capacity and electrical resistivity of a carbon--carbon composite has been measured in the range of 1500 to 3000 K. The melting point of palladium has been measured. Apparatuses for the measurement of thermal expansion and thermal diffusitivity are described. The enthalpy of pure silicon carbide has been measured in the range of 273 to 1200 K. A discussion of the experiments leading to the electronic ground state of FeO is provided. The vibrational spectrum of Boron trimethyl is provided together with the thermodynamic implications.

RESEARCH ON THERMOPHYSICAL PROPERTIES BY DYNAMIC TECHNIQUES

A. Miller, A. Cezairliyan, M.S. Morse

The progress in research on thermophysical properties by dynamic techniques has been in the following four areas.

1. Measurements of specific heat capacity and electrical resistivity of a carbon-carbon composite in the range 1500 to 3000 K
2. Pulse interferometry for thermal expansion measurements
3. Thermal diffusivity apparatus
4. Melting Point of Palladium

In the following sections, progress and results in the above four areas are presented.

1. Specific Heat Capacity and Electrical Resistivity of a Carbon-Carbon Composite in the Range 1500 to 3000 K by a Pulse Heating Method

Considerable effort has been devoted to the design, characterization and testing of a variety of graphite-fiber reinforced composites for a number of applications including the aerospace field where materials with a high strength-to-weight ratio and stability at high temperatures are needed. However, as yet, little attention has been given to non-structural aspects of these materials such as thermal and electrical properties. In the present research, we performed measurements of specific heat capacity and electrical resistivity of a carbon-carbon composite by a pulse heating technique. This technique has been successfully used to study selected thermophysical properties of pure graphite [1] as well as several refractory metals and alloys [2]. Details regarding the pulse technique, the construction and operation of the measurement system, the methods of measuring experimental quantities and other pertinent information, such as the formulation of relations for properties, error analysis, etc., are given in earlier publications [3,4].

The specimen 2-2-3 T-50 carbon-carbon composite consisted of a 3-dimensional orthogonal weave of Thornel 50 graphite fibers impregnated with a matrix of coal tar pitch and graphitized at a processing temperature of 2750°C. Two specimens, in tubular form, were fabricated from a billet furnished by the U. S. Air Force Materials Laboratory.

The response of the high-speed pyrometer was optimized by dividing the temperature interval of the measurements (1500 to 3000 K) into six ranges. Each specimen was then pulse heated in a vacuum environment ($\sim 10^{-5}$ torr) from room temperature successively through each temperature range, beginning with the lowest range. The heating rates varied typically between 3800 and 4300 $K \cdot s^{-1}$. The duration of the current pulse, ranged between 400 and 780 ms. To study possible effects attributable to temperature in the vicinity of the processing temperature (2750°C) of the composite material, each specimen was "heat treated" by an additional 9 heating pulses to 3000 K (2727°C) upon completion of the first series of experiments. The experiments in the successive temperature

ranges were then repeated for each specimen. As will be described later, the heat treatment did not significantly affect the results for specific heat capacity but it did alter the values obtained for electrical resistivity.

The specific heat capacity of the carbon-carbon composite specimens was computed from data taken during the heating period. A correction for the radiative heat loss was based on the results obtained from the initial free cooling of the specimen, following the heating period, during the same experiments. The functions for specific heat capacity that represent the combined results of the two specimens for each series of measurements in the range 1500 to 3000 K are:

For the first series (standard deviation = 0.7%)

$$c_p = 1.691 + 2.598 \times 10^{-4}T - 2.691 \times 10^{-8}T^2 \qquad (1)$$

For the second series (standard deviation = 0.7%)

$$c_p = 1.829 + 1.278 \times 10^{-4}T + 3.876 \times 10^{-9}T^2 \qquad (2)$$

where c_p is in $J \cdot g^{-1} \cdot K^{-1}$ and T is in K. The smoothed values for specific heat capacity computed from equations (1) and (2) are presented at 100 K intervals in Table I. It may be seen that the difference in specific heat values obtained from the first and second series of measurements is less than 1%.

The electrical resistivity of the carbon-carbon composite specimens was determined from the same experiments that were used to calculate specific heat capacity. Unlike specific heat capacity, the results obtained for electrical resistivity were somewhat different for the two specimens, by about 3%. This difference may largely be attributed to anisotropies in the composite material and to differences in the fabrication of the specimens.

The functions for electrical resistivity that represent the combined results for the specimens obtained during the first series of experiments in the range 1500 to 3000 K are (standard deviation = 1.6%):

$$\rho = 733.0 + 6.594 \times 10^{-2}T \qquad (3)$$

where ρ is in $\mu\Omega \cdot cm$ and T is in K.

The second series of measurements, carried out after 10 successive pulse heatings to 3000 K, yielded a significant increase (as much as 5%) in electrical resistivity of the specimens at temperatures below 2900 K; above 2900 K, the resistivity values remained essentially the same as those obtained from the first series of experiments. The functions for

electrical resistivity that represent the combined results for the two specimens obtained in the range 1500 to 2900 K during the second series are (standard deviation = 1.1%):

$$\rho = 878.7 - 1.396 \times 10^{-1}T + 1.549 \times 10^{-4}T^2 - 3.498 \times 10^{-8}T^3 \quad (4)$$

where ρ is in $\mu\Omega$·cm and T is in K. The smoothed values for electrical resistivity obtained from Equations (3) and (4) are given at 100 K intervals in Table I.

Estimates of errors in the measured and computed quantities lead to a value of ±3% as the maximum inaccuracy in both specific heat capacity and electrical resistivity reported in this work. Details regarding the estimates of errors and their combination in experiments with the present measurement system are given in a previous publication [4]. Specific items in the error analyses were recomputed whenever the present conditions differed from those in the earlier publication.

There seems to be no other data in the literature for the thermophysical properties of carbon-carbon composites in the temperature range of our measurements. Consequently, we are using data for a similar material, Poco graphite, as the basis for comparison with our work.

In Figure 1, the specific heat capacity values obtained for the carbon-carbon composite during the first series of experiments are compared with the results for Poco graphite obtained by Cezairliyan and Righini [1] using the same pulse heating system. The difference in our results for the composite and those of Poco graphite is smaller than 1% which is less than the maximum estimated inaccuracy in our measurements (~3%). Similar agreement exists for the specific heat capacity values obtained during our second series of measurements. This agreement suggests that the matrix, in which the graphite fibers are embedded, is essentially graphitic.

The effect of multiple pulse heatings to 3000 K on electrical resistivity is illustrated in Figure 2. It may be seen that resistivity increases with each successive pulse heating, although the magnitude of this increase decreases rapidly with additional pulse heatings. An examination of the specimen surface upon completion of the experiments revealed the existence of microscopic cracks between the yarns containing the graphite fibers and the graphitic matrix. The separations of the

yarn from the surrounding matrix undoubtedly affect the transport properties of the composite in such a way as to increase its electrical resistance. Differences in thermal expansion between fibers and matrix are probably responsible for development of the cracks. In Figure 3, we present our values for electrical resistivity of the composite along with results for two different types of Poco graphite reported earlier [1]. In view of the difference in electrical resistivity (~7%) between different Poco graphite specimens [1], the even larger difference observed between the results for the composite and the Poco graphite is not unusual.

References

1. A. Cezairliyan and F. Righini, Rev. Int. Htes. Temps. et Refract. 12, 124 (1975).

2. A. Cezairliyan, High Temperature Science, in press.

3. A. Cezairliyan, J. Res. Nat. Bur. Stand. 75C, 7 (1971).

4. A. Cezairliyan, M. S. Morse, H. A. Berman and C. W. Beckett, J. Res. Nat. Bur. Stand., 74A, 65 (1970).

Table I. Smoothed specific heat capacity and electrical resistivity for the carbon-carbon composite.

Temperature (K)	Specific Heat Capacity ($J \cdot g^{-1} \cdot K^{-1}$)		Electrical Resistivity ($\mu\Omega \cdot cm$)	
	First Series	Second Series[a]	First Series	Second Series[a]
1500	2.020	2.029	831.9	899.8
1600	2.038	2.043	838.5	908.6
1700	2.055	2.057	845.1	917.2
1800	2.071	2.072	851.7	925.3
1900	2.087	2.086	858.3	932.7
2000	2.103	2.100	864.9	939.3
2100	2.118	2.114	871.5	944.7
2200	2.132	2.129	878.1	948.8
2300	2.146	2.143	884.7	951.4
2400	2.160	2.158	891.3	952.3
2500	2.172	2.173	897.8	951.3
2600	2.185	2.187	904.4	948.1
2700	2.196	2.202	911.0	942.5
2800	2.207	2.217	917.6	934.4
2900	2.218	2.232	924.2	923.4
3000	2.228	2.247	930.8	---

[a] The data for the second series was taken after 10 successive (subsecond) pulse heatings from room temperature to 3000 K.

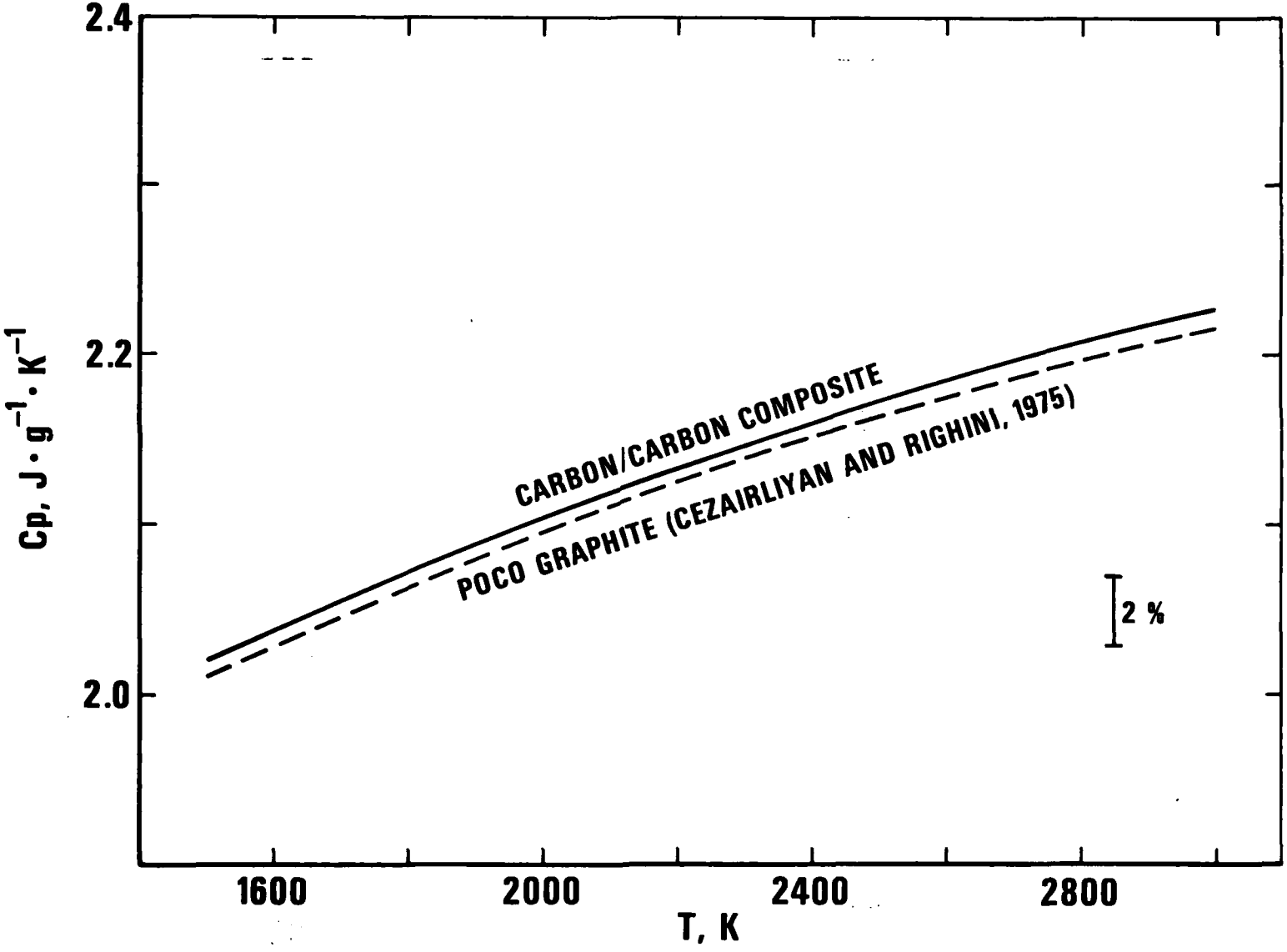

Figure 1. A comparison of specific heat capacity values for the carbon-carbon composite with those obtained by Cezairliyan and Righini [1] for Poco graphite.

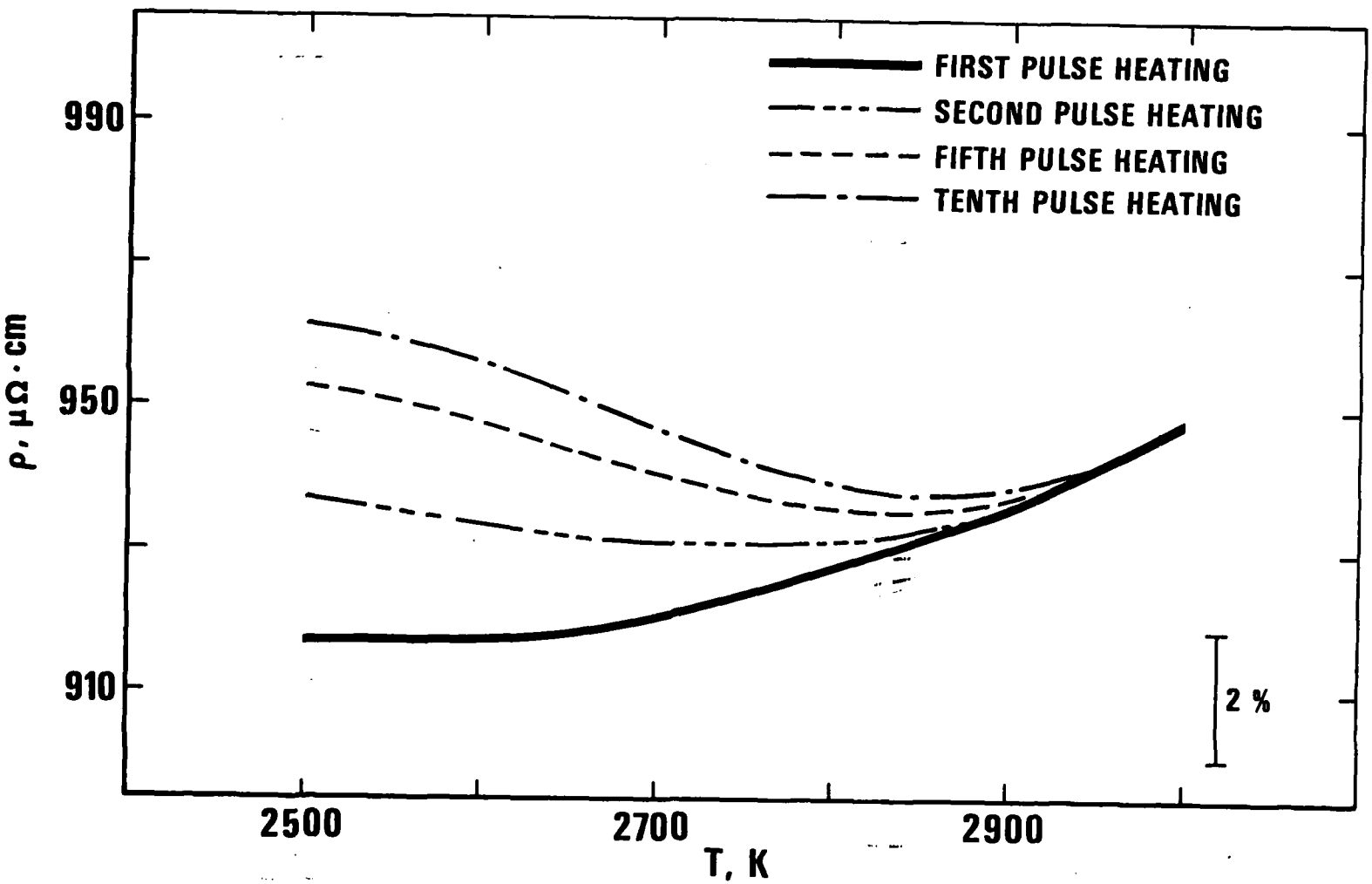

Figure 2. Illustration of the effect on electrical resistivity for the carbon-carbon composite of successive multiple pulse heatings to 3000 K.

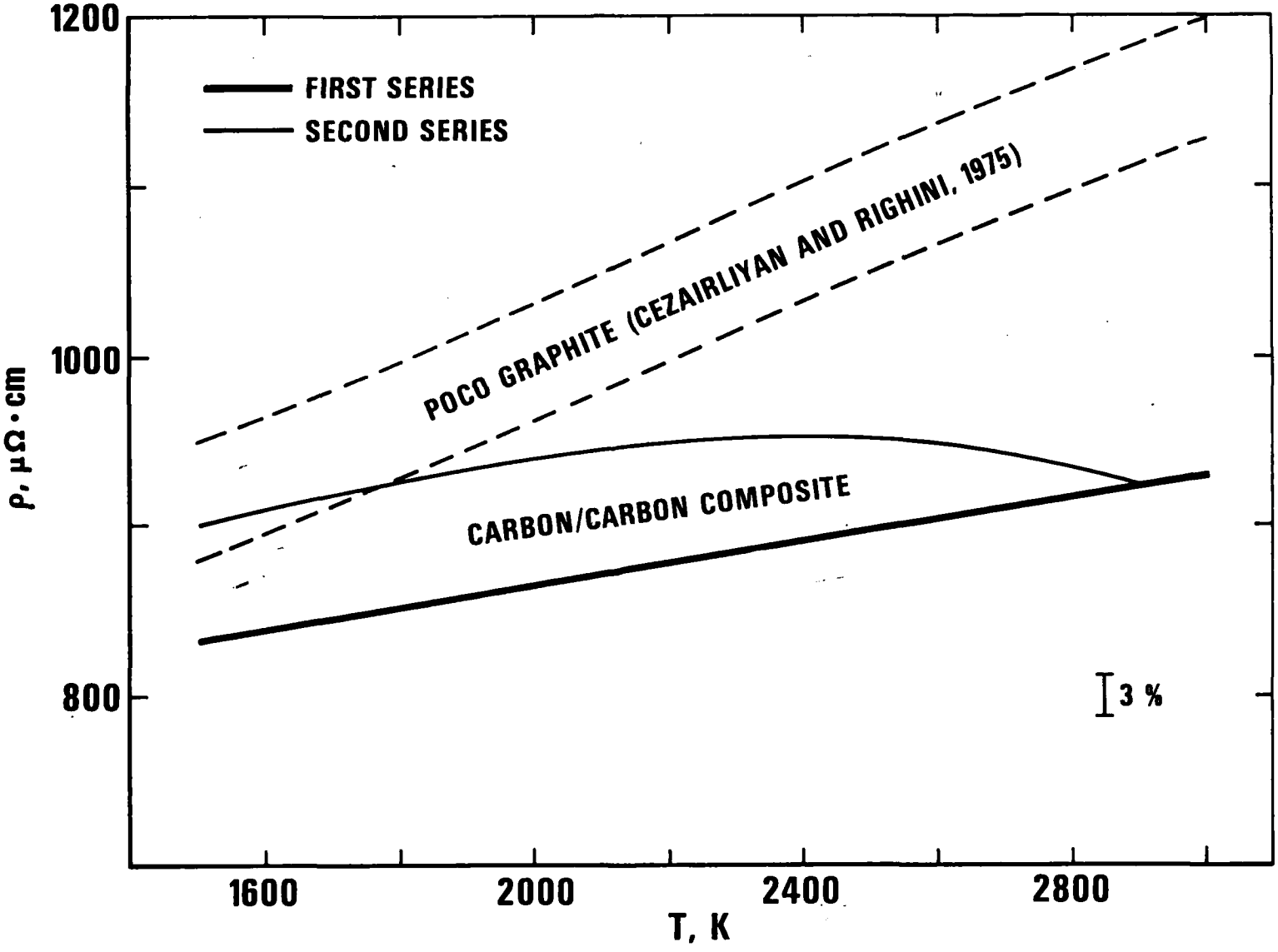

Figure 3. A comparison of electrical resistivity values for the carbon-carbon composite with those obtained by Cezairliyan and Righini [1] for two different types of Poco graphite: AXM-5Q (upper dashed line), DFP-2 (lower dashed line).

2. Pulse Interferometry for Thermal Expansion Measurements

Accurate measurements of thermal expansion based in interferometric methods are generally restricted to temperatures below about 1100 K. At higher temperatures, expansion measurements usually employ other steady-state techniques such as push-rod dilatometry, x-ray diffractometry or the twin-microscope method. In all of these techniques, the specimen is held at elevated temperatures for extended periods of time (minutes to hours) giving rise to problems (increased heat transfer, loss of mechanical strength, evaporation, chemical reactions) which rapidly become more severe with increasing temperature, particularly at temperatures above 2000 K. The effect of these problems can be significantly reduced by using dynamic pulse-heating methods in which the entire experiment is performed in less than one second.

Recently, the feasibility of adapting an interferometer to the NBS pulse heating system for the purpose of measuring thermal expansion of metals at high temperatures was demonstrated [1]. The basic technique involves rapidly heating the specimen from room temperature to temperatures above 1400 K in less than one second by the passage of an electrical current pulse through it and simultaneously measuring the specimen temperature by means of a high-speed photoelectric pyrometer and the shift in the fringe pattern produced by a Michelson-type interferometer: the polarized beam from a He-Ne laser is split into two component beams, one which undergoes successive reflections from optical flats on opposite sides of the specimen, and one which serves as a reference beam.

Preliminary measurements to assess the proposed design were reported earlier [1] and were performed on a long rectangular specimen of tantalum (about 99.9% pure). By recording the pyrometer and interferometer output signals on oscilloscope trace photographs, sufficient information was obtained about the experimental quantities to yield expansivity values at selected temperatures in the range 1400 to 2300 K with an accuracy of better than 3%.

As a result of this preliminary study, a number of modifications have been made to the measurement technique:

(1) The interferometer has been improved by several changes in optical components along the path of the beam reflected by the specimen, as shown in Figure 1. The addition of lenses L1 and L2 (their focal planes coincident with the optical flats on the specimen) eliminates the

translational displacement of the 'specimen' beam at the detector which would otherwise occur if there were (small) rotational movements of the specimen under rapid pulse heating conditions. This ensures that the 'specimen' beam and reference beam remain superimposed at the detector during a pulse experiment. In the earlier version of the interferometer, the beam from the 'front' surface of the specimen was reflected around the specimen by means of corner cubes associated with the polarizing beam splitters PB1 and PB2; however, the alignment of the 'specimen' beam with the reference beam proved to be difficult because of the highly coupled nature of the optical components. This situation has been considerably improved with the addition of the corner cube (C2) - pentaprism (PP2) combination and the mirror (M2) which permit independent translational and angular adjustments, respectively, of the beam reflected by the specimen.

(2) An electronic up/down counter, capable of determining the fringe shift count to the nearest 0.5 fringe, has been constructed and is presently being interfaced with the existing high-speed digital data acquisition system. This modification will permit automatic recording of both the fringe count (every 2.5 ms) and the specimen temperature every 0.833 ms) during rapid pulse heating. The interferometer output signals will also be recorded by a digital-storage oscilloscope (4000 data points) in order to check the interferometer output signals for spurious noise.

(3) Specimens, for subsequent investigations of thermal expansion will be fabricated in the form of precision-machined tubes with two optical flats on opposite sides for the interferometric measurements. A small rectangular sighting hole (fabricated through the wall at the center of each specimen) will permit the direct pyrometric measurement of true (blackbody) temperature of the specimen during dynamic heating to within ±5 K at 2000 K. In the earlier work on tantalum [1], true specimen temperatures were determined from the measured surface radiance on the basis of emittance values in the literature, thereby creating an uncertainty in true temperature as large as ±20 K at 2000 K.

Tubular specimens (with optical flats) have been fabricated from cylindrical rods of tantalum (99.95+% pure). Preparations are now underway to measure the thermal expansion of tantalum at temperatures

in the range 1400 K up to near its melting point (3270 K) during FY 81.

Reference

1. A. P. Miiller and A. Cezairliyan in "Thermal Expansion 6", I. D. Peggs, editor (Plenum, New York, 1978), pp 131-143.

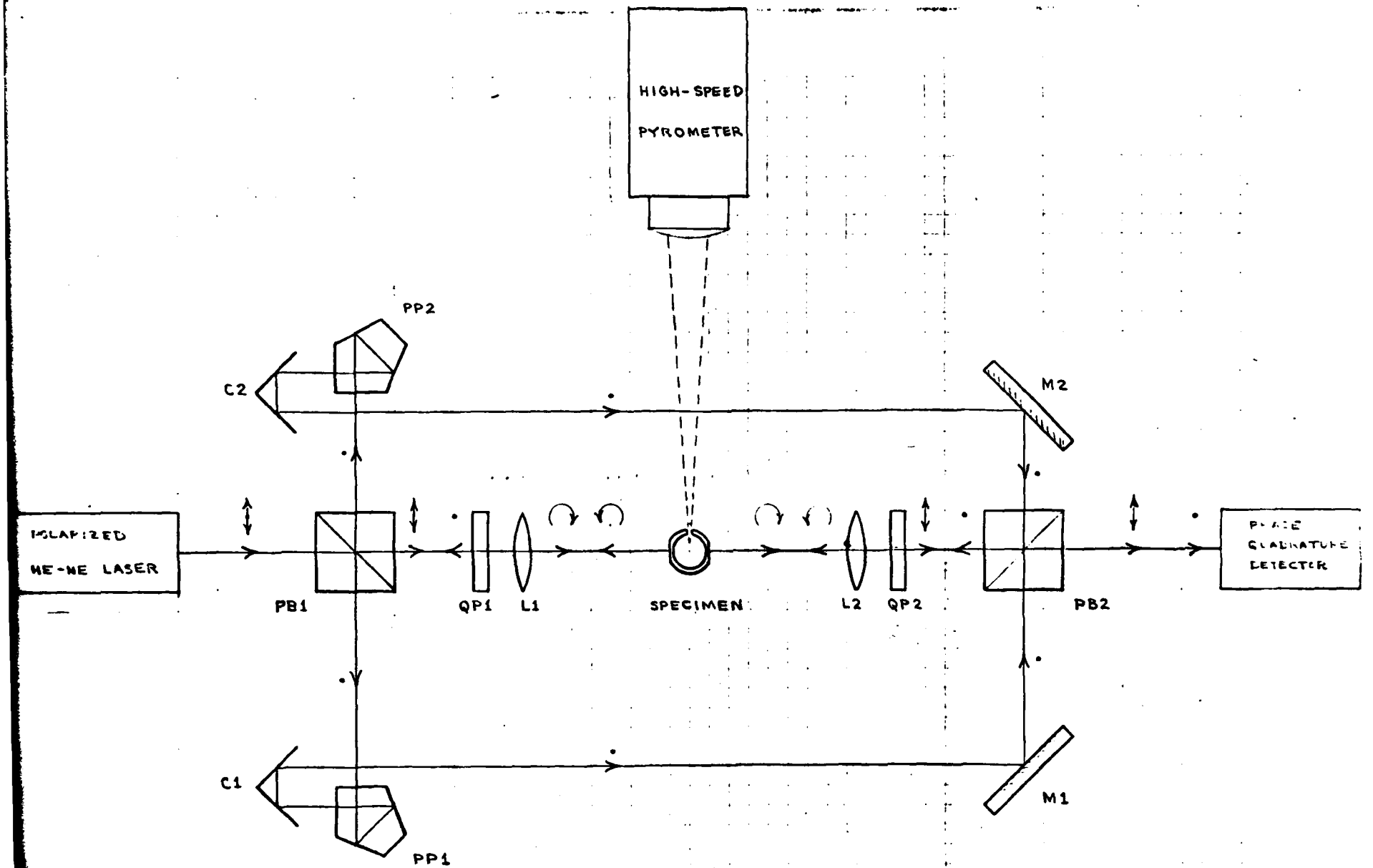

Figure 1: Schematic diagram of the pulse interferometer.

3. Thermal Diffusivity Apparatus

Accurate measurement of thermal conductivity of substances above about 1500 K become difficult if not impossible. An alternate method of obtaining thermal conductivity, λ, is from measurements of thermal diffusivity, α. The relationship is $\alpha = \lambda/\rho c_p$, where ρ is density and c_p is heat capacity.

We are in the process of developing a pulse thermal diffusivity apparatus that utilize a laser pulse to impart energy to the front face of a disc-shaped specimen. The temperature rise at the back face of the specimen is monitored optically. From the temperature-time profile one can obtain the thermal diffusivity of the specimen. The specimen is placed in a tungsten furnace to establish a steady-state base temperature before the laser pulse. Temperature rise at the back face of the specimen due to the laser pulse is of the order of a few degrees. The apparatus is designed for measurements in the temperature range 1500 to 3000 K.

Recently, several modifications and refinements have been made to the apparatus, which included a new optical detection and electronic signal amplification system. The operation of the apparatus was tested by performing preliminary measurements on a Poco graphite specimen. Data on Poco graphite are available in the literature obtained as a part of the AGARD (Advisory Group for Aerospace Research and Development) of NATO program. The results of our measurements were within 10% of those of the earlier work at around 2000 K. This indicates that there were no major errors resulting either from the measurement system or from the method of computations. However, a systematic study of all possible sources of errors, both experimental and analytical, have to be made. This is an important and a critical drawback of almost all reported work in the literature on thermal diffusivity. Particular emphasis needs to be placed on the effect of the departure of actual experimental conditions from the conditions assumed in the formulation of thermal diffusivity. It may be noted that, the thermal diffusivity apparatus under development in our laboratory is the only such apparatus in the U.S. that is capable of measurements to temperatures as high as 3000 K.

4. Melting Point of Palladium

In recent years, the rapid development of high-temperature technologies has required improvements in the methods of determining temperature. Because of the importance of secondary reference points in the calibration of high-temperature sensors, the list of eight secondary reference points above the freezing point of gold given in the text of the International Practical Temperature Scale of 1968 (IPTS-68) [1] was extended in 1977 [2] to seventeen. Of these seventeen, nine secondary reference points (five out of six above 2400 K) are based, at least in part, on measurements by Cezairliyan and co-workers with a pulse heating technique [3,4] in which the entire experiment is performed in less than one second.

The melting point of palladium is listed as a secondary reference point on the IPTS-68 with a value of 1827 K. The listed value is based on a conversion to the IPTS-68 of three experimental determinations [5,7] obtained about fifty years ago by visual optical pyrometry. In the present work, an independent redetermination of the melting point of palladium has been carried out by a rapid pulse heating technique in which temperature is measured with a high-speed photoelectric pyrometer. The short measurement time (less than one second) of our technique tends to minimize the problems associated with quasi steady-state experiments, in particular, specimen evaporation which, in the case of palladium, is enhanced by the relatively high vapor pressure near its melting point.

The experiments were performed on three tubular specimens fabricated from cylindrical rods of palladium (99.95+% pure) by an electro-erosion technique. Approximate blackbody conditions for pyrometric temperature measurements were achieved by means of a rectangular sighting hole fabricated through the wall at the middle of each tube. Each specimen was resistively heated in an argon environment at about 0.2 MPa (~2 atm.) from room temperature to the melting point by the passage of an electrical current pulse through it. The duration of the current pulse varied from 550 to 600 ms. The corresponding heating rates ranged between 3740 and 3570 $K \cdot s^{-1}$.

In determining the specimen temperature from the measured spectral radiance, corrections were made to account for the departure of the

specimen from true blackbody conditions and for the light scattering effect of the optics in the pyrometer. Based on geometrical considerations only, the blackbody quality of the specimen was estimated to be 0.98 by De Vos' [8] method. The 2% correction in radiance corresponds to an upward correction in temperature of 3.1 K at 1800 K. For the pyrometer/specimen configuration of the present work, 1.2% of the measured radiance comes from the specimen surface surrounding the blackbody radiation hole. Normal spectral emittance of the specimen near its melting point is about 0.4 at 0.65 μm, effective wavelength of the pyrometer [9]. A correction to measured radiance for scattered light, taking into account the emittance of the specimen surface, yields an upward correction in temperature of 1.1 K at 1800 K.

The results on melting temperature are summarized for each specimen in Table I. The average melting temperature for the three specimens is 1826.9 K with an average absolute deviation from the mean of 0.1 K. It may be concluded that the melting point of palladium as determined by our measurements is 1827 K.

Table I. Experimental results for the melting point of palladium.

Specimen number	Heating rate[a] $K \cdot s^{-1}$	Number of temp. at plateau	Melting pt. K	Standard dev. K
1	3740	31	1827.1	0.3
2	3600	15	1826.8	0.3
3	3570	41	1826.9	0.4

A detailed analysis of the sources and magnitudes of errors involved in the measurement of specimen temperature with the NBS pulse heating system has been given in an earlier publication [4]. Specific items in the analysis were recomputed whenever the present conditions differed from those in the earlier publication. The error contributions to the measurement of temperature in the present work arising from the reference lamp, the pyrometer and the specimen are estimated to be not more than ±4 K.

The value of 1827 ±4 K obtained in the present work by a pulse heating method (heating rate ~ 10^4 K·x^{-1}) is the same as the accepted value for the palladium melting point (1827 K) based on quasi-steady state experiments. This agreement strengthens the basis for the secondary reference points above 1800 K which were determined from measurements by dynamic techniques.

References

1. The International Committee for Weights and Measures, Metrologia 5, 35 (1969).
2. L. Crovini, R. E. Bedford and A. Moser, Metrologia 13, 197 (1977).
3. A. Cezairliyan, J. Res. Natl. Bur. Stand. (U.S.A.) 75C, 7 (1971).
4. A. Cezairliyan, M. S. Morse, H. A. Berman and C. W. Beckett, J. Res. Natl. Bur. Stand. (U.S.A.) 74A, 65 (1970).
5. C. O. Fairchild, W. H. Hoover and M. F. Peters, J. Res. Natl. Bur. Stand. (U.S.A.) 2, 931 (1929).
6. F. H. Schofield, Proc. Roy. Soc. (London) A125, 517 (1929).
7. F. H. Schofield, Proc. Roy. Soc. (London) A155, 301 (1936).
8. J. C. DeVos, Physica 20, 669 (1954).
9. A. P. Miiller and A. Cezairliyan, High Temperature Science, 11, 41 (1979).

Enthalpy of Pure Silicon Carbide

D. A. Ditmars

Introduction

Pure silicon carbide, a semiconductor material chemically stable at elevated temperatures, also possesses a sufficient degree of strength, hardners and thermal conductivity to make it attractive for application in components of systems operating at high temperatures (near 1500 K) and in highly reactive atmospheres. It exists in several allotropic modifications, the principal ones being α-SiC (hexagonal) and β-SiC (cubic, or diamond-type lattice), formed at high temperatures.

About five high-temperature heat-capacity studies of silicon material and most are flawed by uncertainty as to the phase composition or by a high impurity level. We are contributing to an improvement in the high temperature heat capacity data for SiC through heat measurements on single-crystal specimens of SiC of the highest purity attainable, in the range from room temperature up to the decomposition range (reportedly, above 2100 K). The present report gives our preliminary results obtained in the temperature range 273-1173 K.

Samples

Several samples of single-crystal silicon carbide were obtained from the Carborundum Company (Niagra Falls, N.Y.) and from Atomergic Chematols Corporation (Plainview, N.Y.) Dr. E. Kraft of the Research and Development Division of The Carborundum Company supplied eight samples representing material of the highest purity from a special Carborundum Co. research project and from their production-type Acheson furnaces. Two samples of this material were chosen and labeled "SiC-III" and "SiC-V". The Atomergic Chemicals sample was labeled "SiC-I". These three samples were first examined in NBS labs by X-ray powder diffraction analysis and by semiquantitative spectroscopic analysis. In addition, quantitative analyses were performed for total carbon, free carbon, and total silcon.

The X-ray analyses of the three samples showed them to be structurally identical, homogeneous, of the α-polytype, and detected no impurity phases. The spectroscopic and the quantitative analyses, while not in exact agreement, indicated that each of the three samples contain at most 0.7% impurities and no more than 0.05% free carbon. For the purpose of these preliminary results, the samples will be treated as stoichiometric SiC (M.W. = 40.096).

Method

The samples were encapsulated in Pt-10Rh alloy capsules with an interior atmosphere of helium at a pressure of about 15 mmHg. Relative enthalpy measurements were made in the same Bunsen ice calorimeter used in prior heat-capacity studies by NBS under AFOSR contracts. In this calorimeter, the sample in its capsule is heated to a constant, measured temperature in a resistance furnace and then suddenly dropped into the calorimeter. Here, the enthalpy, relative to the ice point, of the sample plus capsule is measured by measuring the volume change within the calorimeter as the heat from the cooling sample melts ice within the calorimeter. This volume change is expressed in energy units by means of an electrical calibration of the calorimeter. Finally, the relative enthalpy of the capsule material itself is measured in a similar fashion in a separate experiment. During these measurements on SiC, occassional measurements on a heat-capacity standard reference material (α-Al_2O_3) were made to ensure correctness of the experimental technique and of the calorimeter functioning.

Results

Heat measurements on the standard reference material (NBS SRM-720) were made at the temperatures 373K, 573K, 773K, and 973K, interspersed throughout the chronological course of the SiC measurements. These showed excellent precision (range <0.06% for duplicate heat measurements at all temperatures) and accuracy (maximum deviation from ethalpy of SRM 720 = 0.03%.

The raw enthalpy data for the SiC samples are presented in the accompanying table. These data are now being analyzed and compared with existing literature data. Measurements on these same samples at higher temperatures will be made in an adiabatic receiving calorimeter. These measurements have been postponed pending the receipt of an improved automatic optical pyrometer.

Preliminary Enthalpy Data for SiC

Exp. No.	T / K	Capsule + Sample $H_T - H_{273.15}$ / J	Capsule $H_T - H_{273.15}$ / J	Sample $H_T - H_{273.15}$ / J/Mole
595	376.713	664.68	188.25	3040.95
603	574.320	2220.37	562.95	10573.51
608	772.661	3987.52	953.08	19353.83
624	973.89	5895.95	1362.62	28910.54
616	326.881	293.49	96.67	1478.99
617	326.894	291.78	96.70	1465.96
590	376.511	592.24	187.88	3038.18
591	376.583	590.71	188.01	3025.73
592	376.628	591.81	188.09	3033.36
597	472.114	1378.71	367.18	7596.43
598	471.754	1377.15	366.50	7589.81
599	471.679	1375.93	366.36	7581.70
600	574.095	1970.16	562.52	10572.93
601	574.071	1969.23	562.47	10566.32
602	574.081	1969.66	562.49	10569.43
629	574.081	1964.94	562.49	10534.00
586	668.992	2701.80	747.53	14677.62
587	668.972	2702.01	747.49	14679.44
588	669.038	2703.95	747.62	14693.06
589	772.995	3541.52	953.75	19434.34
609	772.889	3537.46	953.54	19405.41
610	772.701	3536.73	953.16	19402.76
612	872.10	4354.83	1153.68	24039.94
613	872.18	4360.63	1153.84	24082.22
614	872.19	4358.30	1153.86	24064.61
621	964.98	5134.60	1344.19	28464.52
622	965.03	5129.26	1344.29	28.423.75
623	973.93	5219.94	1362.70	28966.16
625	1072.74	6073.89	1569.23	33827.30
626	1072.48	6062.03	1568.69	33742.44
627	1072.56	6063.75	1568.86	33754.05
628	1072.61	6031.22	1568.97	33509.38

Preliminary Enthalpy Data for SiC (Cont.)

Exp. No.	$\frac{T}{K}$	Capsule + Sample $\frac{H_T - H_{273.15}}{J}$	Capsule $\frac{H_T - H_{273.15}}{J}$	Sample $\frac{H_T - H_{273.15}}{J/Mole}$ [1]
596	376.571	617.77	187.99	2990.45
584	473.929	1297.71	370.63	6450.29
575	470.061	1270.09	363.29	6309.15
577	470.061	1272.52	363.29	6326.07
578	569.120	2009.25	552.90	10132.39
579	569.242	2002.70	553.14	10085.20
580	569.164	2028.19	552.98	10263.52
582	672.291	2857.67	754.02	14635.49
583	672.228	2863.55	753.89	14677.29
585	668.918	2829.72	747.38	14487.18
611	772.566	3706.89	952.89	19159.72

[1] M.W. = 40.096

The Assignment of the Electronic Ground State of FeO

Stanley Abramowitz

The use of matrix isolation spectroscopy as an aide to the identification of ground electronic states is well known. The symmetry and degeneracy of the electronic ground state is very important for thermodynamic calculations. In a recent paper Green Reedy and Kay reported on the infrared spectra of the isotopic species of FeO isolated in an Ar matrices at 14K (1). The results of this work indicated that the ground state constants of FeO are ω_e = 880.02 and $\omega_e x_e$ = 3.47cm^{-1}. These results are in agreement with previous results reported by Abramowitz, Acquista and Levin (2) who in a study of the matrix isolated spectra of FeO_2 formed from reactions of Fe(v) with N_2O observed a peak at 873cm^{-1} attributed to FeO. Barrow and Senior have done some rotational analysis of the orange system of FeO. In this work they identify the lower state as a $^5\Sigma$ or $^7\Sigma$ with ω_e'' = 880.53cm^{-1} and $\omega_e'' x_e''$ = 4.63 (3). This system has also been seen in absorption following flash heating of Fe in the presence of oxygen (4, 5). The same system has been seen in the chemiluminescence attendant upon the reaction of Fe(v) with N_2O and O_3 (6). These experiments involving the use of several techniques have led Green, Reedy and Kay to assign the ground electronic state to a $^5\Sigma$.

There are however other experiments which in an equally convincing manner assign the lower state of FeO to a state having ν_o = $\sim$ 940cm^{-1}. Engleking and Lineberger using photoelectron spectroscopy technique report a $^5\Delta$ ground state for FeO with a vibrational frequency of 970 $\pm$ 60cm^{-1} (7). On the basis of this measurement it was argued that the ground state of FeO is the previously assigned D state with a ω_e = 955cm^{-1}. They also observed the first excited state of FeO with To $\sim$ 3990cm^{-1} and a ν_o of 900 $\pm$ 100Cm^{-1}. The recent compilation of the evaluated data for diatomic molecules supports this assignment (8). DeVore and Gallaher have observed a vibration rotation spectrum of a species formed by passing an oxygen-argon mixture over heated $FeCl_3$ and into a microwave discharge (9). They observed some Q branches and structure which have been interpreted to yield ν_o = 943cm^{-1} and Be = 0.546cm^{-1}. These spectroscopic constants are in reasonable agreement with those of the previously assigned D state of FeO. They could not resolve the multiplet structure expected for a quintet or septet state. However, the appearance of a Q branch does indicate a Δ and not a Σ state.

There are two ab-initio calculations for FeO that indicate the ground electronic state is a $^5\Delta$ with the first excited level a $^5\Sigma$ (10, 11). The calculation given in reference 10 appears to be quite detailed and exhaustive. Another calculation the results of which are quoted in reference 6, indicate a $^5\Sigma$ ground state (12). Finally the absence of an electron spin resonance spectrum for matrix isolated FeO can be interpreted as being supportive of the assignment of $^5\Delta$ ground state (13).

It may very well be that all these experimental results are consistent. If FeO has a low lying electronic state (indeed the photodetachment studies indicate $^5\Sigma - {}^5\Delta \sim 3990cm^{-1}$) then one may not be able to draw conclusions from gas phase absorption spectroscopic studies. This will be particularly true if one uses a "chemical" method of production of the species eg. Fe + N_2O, Fe + O_3 or $Fe(CO)_5$ + O_2 or Fe + O_2. In particular the heats of these chemical reactions may be ample to populate low lying excited electronic states. In this connection it should be noted that the reaction Fe + O_2 is endothermic and doesn't go easily. Only the FeO_2 spectrum was found in the research on the matrix isolated products of the reaction of Fe + O_2. The system used by West and Broida involves many collisions before the observations are made.

It should also be noted that FeO has a large dipole moment. The ab-initio calculation indicates a dipole momemnt of about 7·9 Debye. This yields a charge separation (μ_e/er_e) of 0.96. This is to be compared with experimental μ_e/er_e of 0.85, and 0.84 for BaO and LiF. These species exhibit shifts of ν_o in going from the gas phase to argon matrices of 32 and $56cm^{-1}$. Coupling the shift expected in argon matrices with the uncertainties in ν_o from the photodetachment studies indicates the $873cm^{-1}$ observed for matrix isolated ν_o of FeO is not necessarily in disagreement with the $970 \pm 60cm^{-1}$ quoted for FeO in the gas phase.

Recently Vala, Brittain and Powell have shown that it is possible to assign the symmetries of matrix isolated high temperature diatomic molecule species using the method of magnetic circular dichroism (14). Using this method they have investigated several high temperature species including TiO, HfO, VO, NbO and TaO in argon matrices at cryogenic temperatures. They have been able to confirm the ground state of TiO as $^3\Delta_r$ and also assign symmetries for the transition. Similar results have also been reported for Mg_2 and Ca_2 (15). Consequently it is clear that the observation of the magnetic circular dichroism spectrum of matrix isolated FeO should differentiate between a $^5\Delta$ and $^5\Sigma$ ground state. Alternatively the observation of a completely resolved electronic spectrum of FeO would allow a difinitive choice of the ground state.

REFERENCES

1) D.W. Green, G.T. Reedy, J.G. Kay, J. Mol. Spectroscopy 78, 257 (1974).

2) S. Abramowitz, N. Acquista, I.W. Levin, Chem. Phys. Letters 50. 423, (1977).

3) R.F. Barrow and M. Senior, Nature (London) 223, 1350 (1969).

4) A.M. Bass, N.A. Kuebler, L.S. Nelson, J. Chem. Phys. 40, 3121 (1964).

5) J.G. Kay, K.E. Bartlett, D.M. Byler, as cited in reference 1.

6) J.B. West and H.P. Broida, J. Chem. Phys. 62, 2566 (1975).

7) D.C. Engleking and W.C. Lineberger, J. Chem. Phys. 66, 5054 (1977).

8) K.P. Huber and G. Herzberg, Molecular Spectra and Molecular Structure IV Constants of Diatomic Molecules, Van Nostrans Reinhold Co., New York 1979 p. 221.

9) T.C. DeVore and T.N. Gallaher, J. Chem. Phys. 70, 4429 (1979).

10) P.S. Bagus and J.H.T. Pearson, J. Chem. Phys. 59, 2986 (1973).

11) S.P. Walch and G.T. Goddard III, unpublished results (see reference 4 of reference 10).

12) H.H.Michels, unpublished result (see reference 17 of reference 6).

13) W. Weltner, Jr., Ber. Bunsengeschellschaft, 82, 80 (1978).

14) R. Brittain, D. Powell, E. Voigtman, M. Vala, Rev. Sci. Inst. 80, 905 (1980).
R. Brittain, D. Powell, M. Kreglewski, M. Vala, Chem. Phys. 80, 71 (1980).

15) A.C. Miller, E.R. Karusz, S.M.Jacobs, H. W. Kim, P.N. Schatz, L. Andrews, paper 106 ACS Meeting September 1979, Washington, D.C.

Vibrational Spectrum of and Thermodynamic Properties of $B(CH_3)_3$

Stanley Abramowitz

Introduction

The infrared and Raman spectra of gaseous Boron trimethyl have been reinvestigated. The object of this study was to compare the third law entropy of this complicated species with the experimentally measured entropy (1). Boron trimethyl has a BC_3 planar Sheleton. The symmetry of the molecule depends upon whether the CH_3 groups rotate freely. Conventional point group theory would indicate a D_{3h} symmetry for freely rotating CH_3 groups (2). It will be shown that the observed spectra can be better explained by the G_{324} molecular symmetry group based upon the molecular symmetry group theory first proposed by Longuet-Higgins (3,4). A program was developed to compute the thermodynamic functions for anharmonic oscillators. Somewhat better agreement between the computed third law entropy and that determined experimentally is obtained by considering vibrational enharmonicity.

Experimental

The Boron trimethyl used was from the same sample used for the low temperature calorimetry measurements (1). An investigation of its infrared spectrum did not show any impurities. Raman spectra were observed using a conventional monochromator equipped with a stepping motor drive and photon counting electronics. The spectrometer is interfaced with a dedicated minicomputer which both operated the instrument and stored the data. A typical spectrum was run at a spectral slit width of $2cm^{-1}$ using an Argon ion gas laser excitation with a power level of about 4W in the 514.5mm line. A survey spectrum is shown in Figure 1 for both parallel and perpendicular polarizations. The infrared spectra were observed using a commercial double beam optical null instrument. Spectal slit widths of about $1cm^{-1}$ were used to observe the vibration rotation band contours.

Results and Discussion

The vibrational modes of $B(CH_3)$ are shown in Table 1. For a D_{3h} symmetry one expects 20 normal modes for freely rotating methyl groups. The A_1', E' and E'' modes are Raman active while the A_2'' and E' modes are infrared active. If one considers the G_{324} molecular symmetry group there are 15 normal modes with A_1, G and E_2 Raman active while A_3, I, G and E_2 are infrared active. Table 1 shows a correlation diagram between D_{3h} and G_{324} symmetries. It should be noted that G_{324} requires 8 Raman active modes and nine infrared active modes while D_{3h} symmetry requires 13 Raman active modes and 11 infrared active modes. The significant feature of the MS group is the relative simplicity of the expected vibrational spectrum. The observed vibrational spectra in both the infrared and Raman confirm the MS symmetry group as the better representation of this "species" symmetry. The Raman spectra of gaseous $B(CH_3)_3$ are shown in figures 1-5. In all cases both parallel and perpendicular polarizations are given. Those vibrations which are totally symmetric (ν_1, ν_2, and ν_3) are polarized. Infrared spectra are shown in Figures 6 and 7. The BC_3 asymmetric stretch ν_{15} for D_{3h} and ν_{14} for G_{324} symmetries respectively shows a ^{10}B-^{11}B isotope shift of about 30 cm^{-1}. This shift is to be expected for a planar BC_3 skeleton. (The corresponding mode in the boron trihalides also show a large isotope shift.) Three out of the four A_3 modes have the same P-R separation which is to be expected for these parallel transitions. These modes are also as expected not present in the Raman spectrum. The three A_1 modes at 2916, 1291 and 678cm^{-1} are all polarized and not present in the infrared spectrum as required by the selection rules. The two 6 fold degenerate vibrations ν_{11} and ν_{12} have rather broad unstructured contours in both the infrared and Raman spectra. In summary the infrared and Raman spectra are consistent with a G_{324} molecular symmetry assignment. These are not enough vibrational bends observed to justify a D_{3h} assignment for the $B(CH_3)_3$ molecule. A summary of the vibrational assignment is given in Table 2.

A calculation of the third law entropy of $B(CH_3)_3$ can be made using the rigid rotor harmonic oscillator approximation and assuming free rotation of the three methyl groups about the B-C bonds. The vibrational assignment given in Table 2 is used toether with the bond distances and angles determined using electron diffraction techniques by Bartell and Carroll (5). An entropy of 67.83 cal/K at 199.92 K is computed.

This compares with the measured value of 68.29 $\pm$ 0.10 cal/K (1). The fact that the measured entropy is greater than that computed using spectroscopic data indicates essentially free rotation of the methyl groups. Any significant barrier to the rotation of the methyl groups results in a lowering of the calculated entropy and therefore an increase in the discrepancy between the measured and computed entropy.

A computer program has been written to compute the effect of anharmonicity on the vibrational contribution to the entropy. In this computation all vibrational states were assumed to have a 1% anharmonicity (other values of the anharmonicity can be chosen). This computer code obtains a state sum by counting those levels whose partition coefficient exceeds a chosen value in this case 10^{-8}. A choice of 10^{-11} does not effect the computed entropy. An increase of 0.03 e.u. is obtained in this manner. The projected error increases for higher temperatures.

This program will be especially useful in computing estimated errors in entropy caused by vibrational anharmonicity. It will therefore be useful for comparing third law (statistically calculated) entropies with those derived from thermodynamic measurements. By identifying expected differences the evaluation of thermodynamic data particularly for high temperature species should be expedited.

REFERENCES

1) Furukawa, G.T. and Park, R.P. National Bureau of Standard Report 3644 (1954).

2) Woodward, L.A., Hall, T.R., Dixon, R.N., Sheppard, N., Spectrochim. Acta 15, 249 (1959).

3) Longuet-Higgins, H.C., Molecular Phys. 6, 445 (1963).

4) Bunker, P.R., Molecular Symmetry and Molecular Structure, Academic Press, New York (1979).

5) Bartell, L.S., and Carroll, B.L., J. Chem. Phys. 42, 3076 (1965).

Table 1. Correlation Table for D_{3h}-G_{324} and for $B(CH_3)_3$

Point Group D_{3h}				Molecular Symmetry Group G_{324}		
Species	Vibration	Activity	Mode	Vibration	Species	Activity
A_1'	1	R(p)	CH_3stretch	1	A_1	R(p)
	2		CH_3deformation	2		
	3		BC_3stretch	3		
A_2'	4	IA	CH_3stretch	4	A_4	IA
	5		CH_3deformation	5		
	6		CH_3rock	6		
A_2''	7	IR	CH_3stretch	7	A_3	IR
	8		CH_3deformation	8		
	9		CH_3rock	9		
	10		BC_3deformation	10		
E'	11	IR,R	CH_3stretch	11		
	12		CH_3stretch			
	13		CH_3deformation	12		
	14		CH_3deformation			
	15		BC_3stretch			
	16		CH_3rock	13	G	IR,R
	17		BC_3deformation			
E"	18	R,R	CH_3stretch	14		
	19		CH_3deformation			
	20		CH_3rock	15	E_2	IR,R

Table 2. Vibrational Assignment of B(CH3)3 According to G324 MS Group

Species	Vibration	IR	Raman	Inactive (Estimate)
A_1	1		2916	
	2		1291	
	3		678	
A_2	4			2915
	5			1400
	6			900
A_3	7	2914		
	8	1303		
	9	975		
	10	326		
I	11	2984	2985	
	12	1450	1445	
G	13	867	868	
E_2	14	1184	1162	
		1154		
	15	310	314	

FIGURE 1

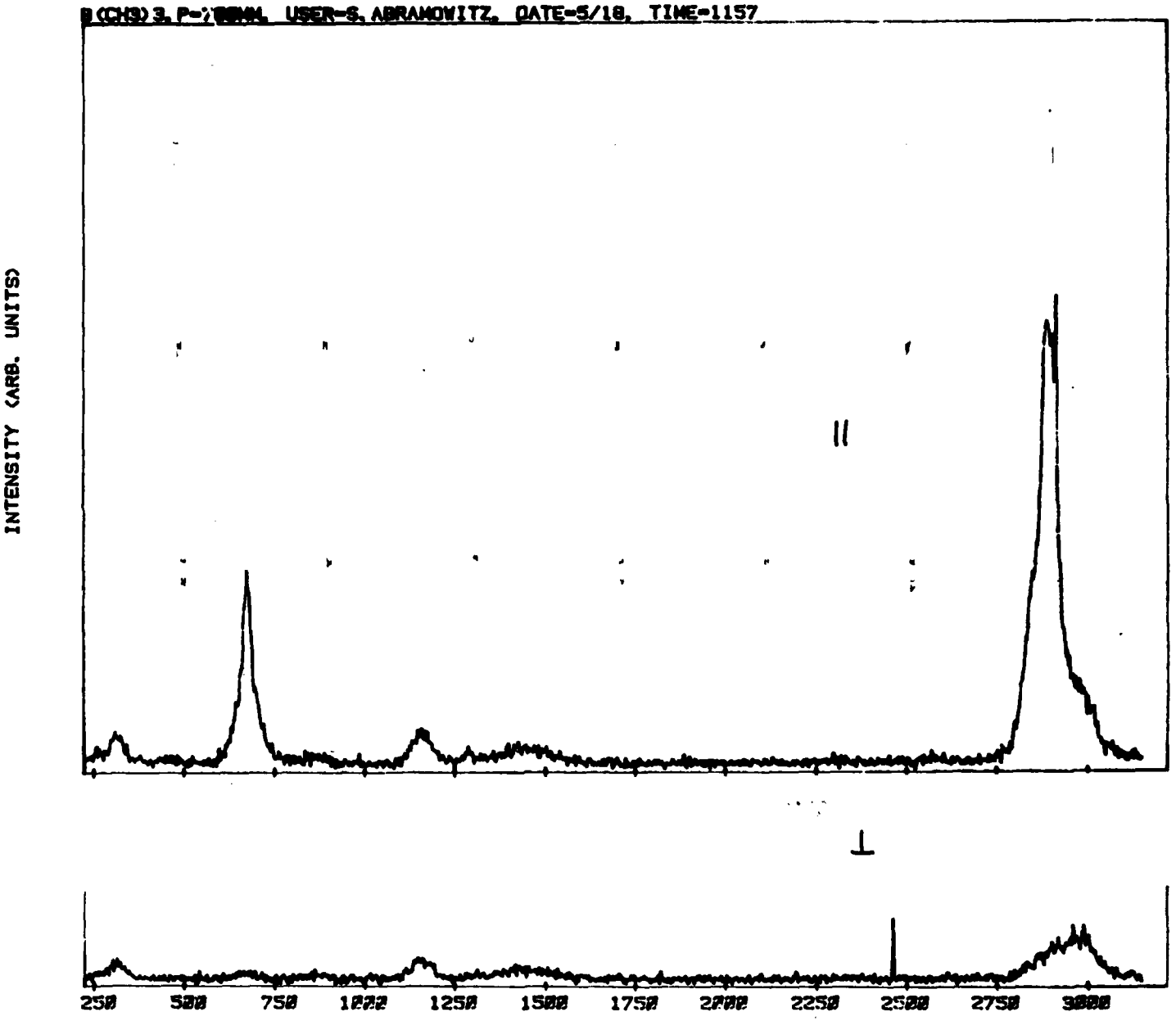
B(CH3)3, P=?, USER=S. ABRAMOWITZ, DATE=5/18, TIME=1157
INTENSITY (ARB. UNITS)
II
⊥
250
500
750
1000
1250
1500
1750
2000
2250
2500
2750
3000

FIGURE 2

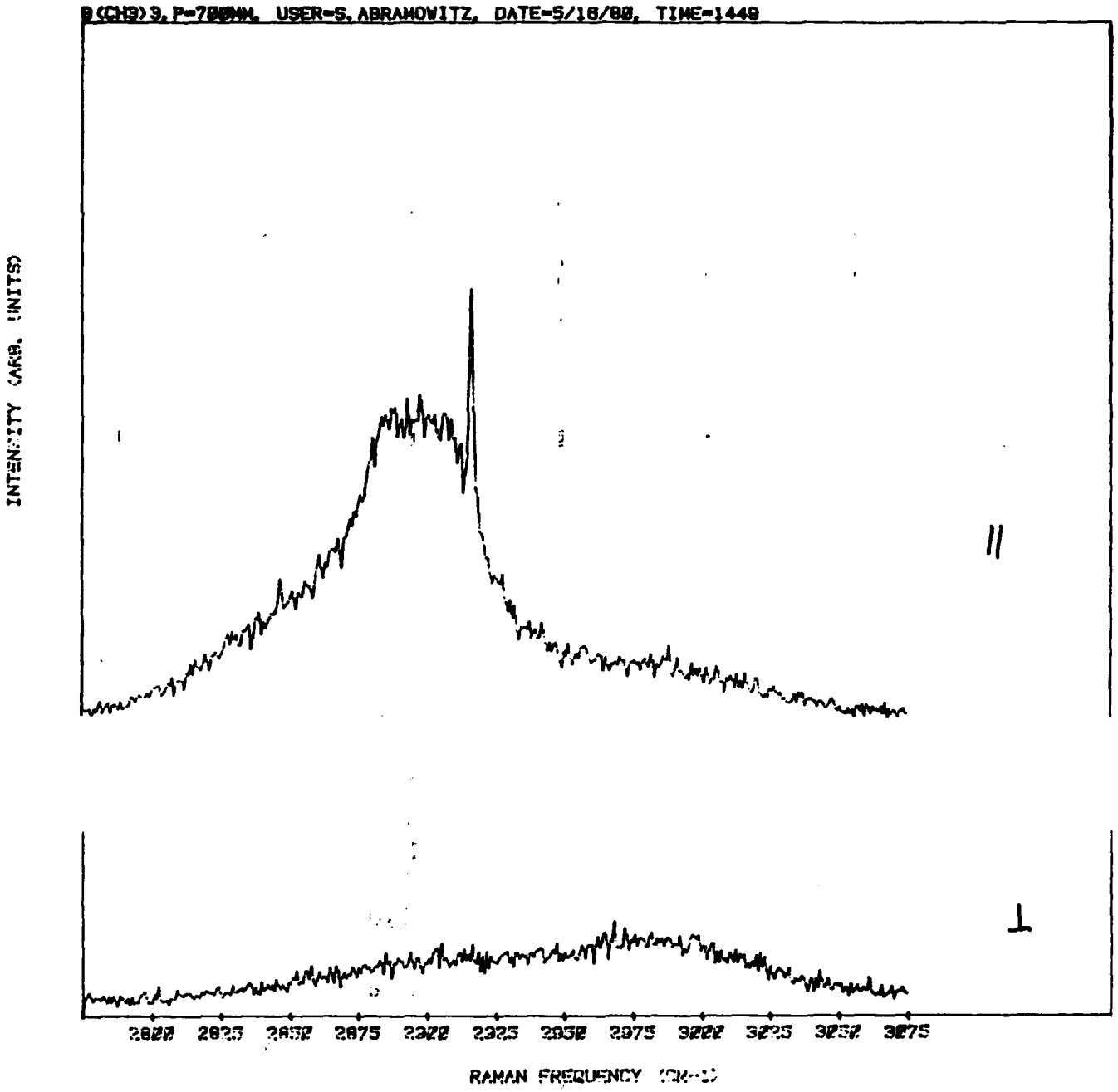
9(CH9) 9, P=700MM, USER=S. ABRAMOWITZ, DATE=5/16/80, TIME=1449
INTENSITY (ARB. UNITS)
||
⊥
2822
2925
2952
2975
3222
3225
3252
3275
RAMAN FREQUENCY (CM--1)

FIGURE 3

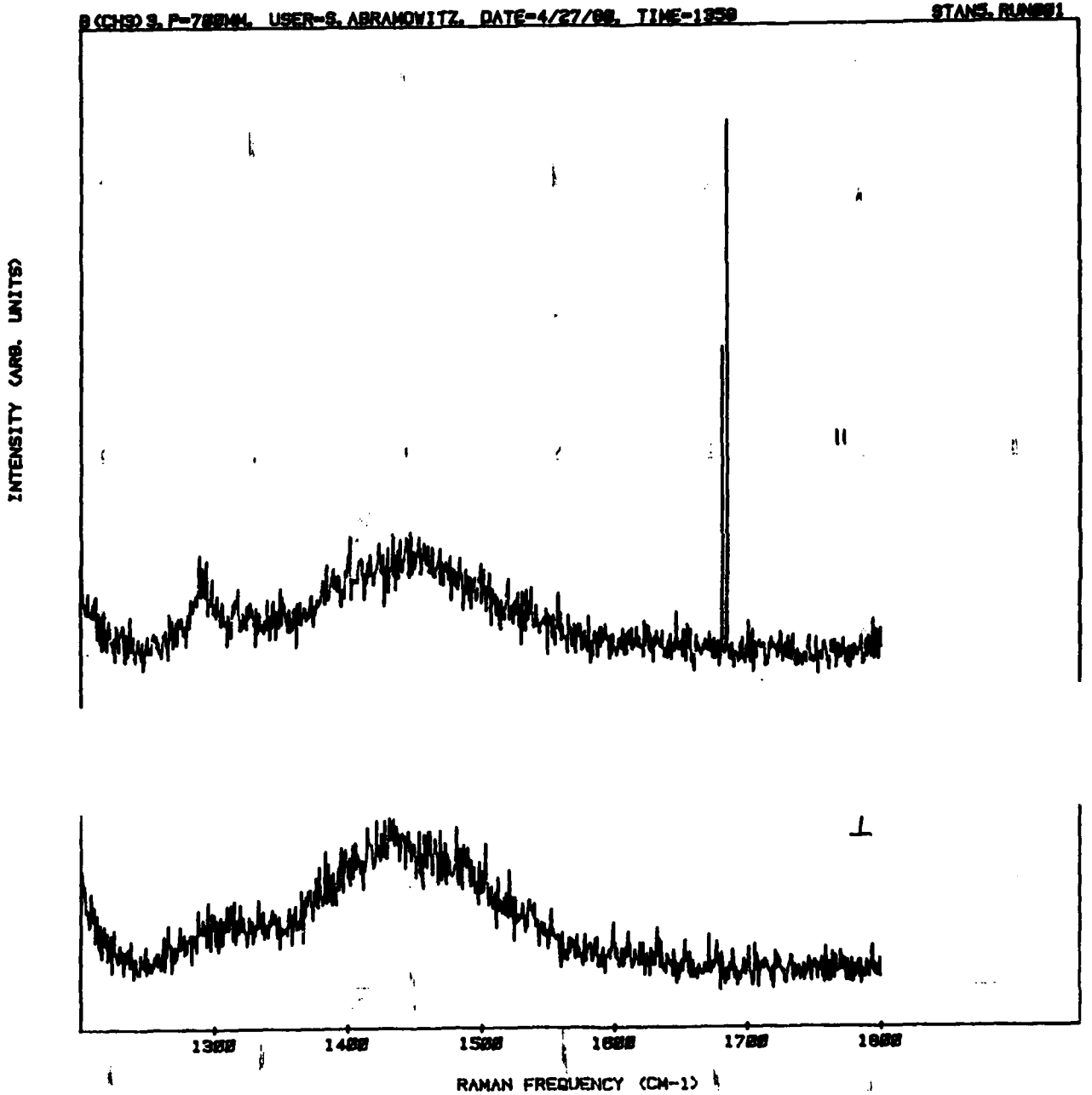
B(CH3)3, P=700MM, USER=S. ABRAMOWITZ, DATE=4/27/88, TIME=1350
STAN5.RUN001
INTENSITY (ARB. UNITS)
II
⊥
1300
1400
1500
1600
1700
1800
RAMAN FREQUENCY (CM-1)

FIGURE 4

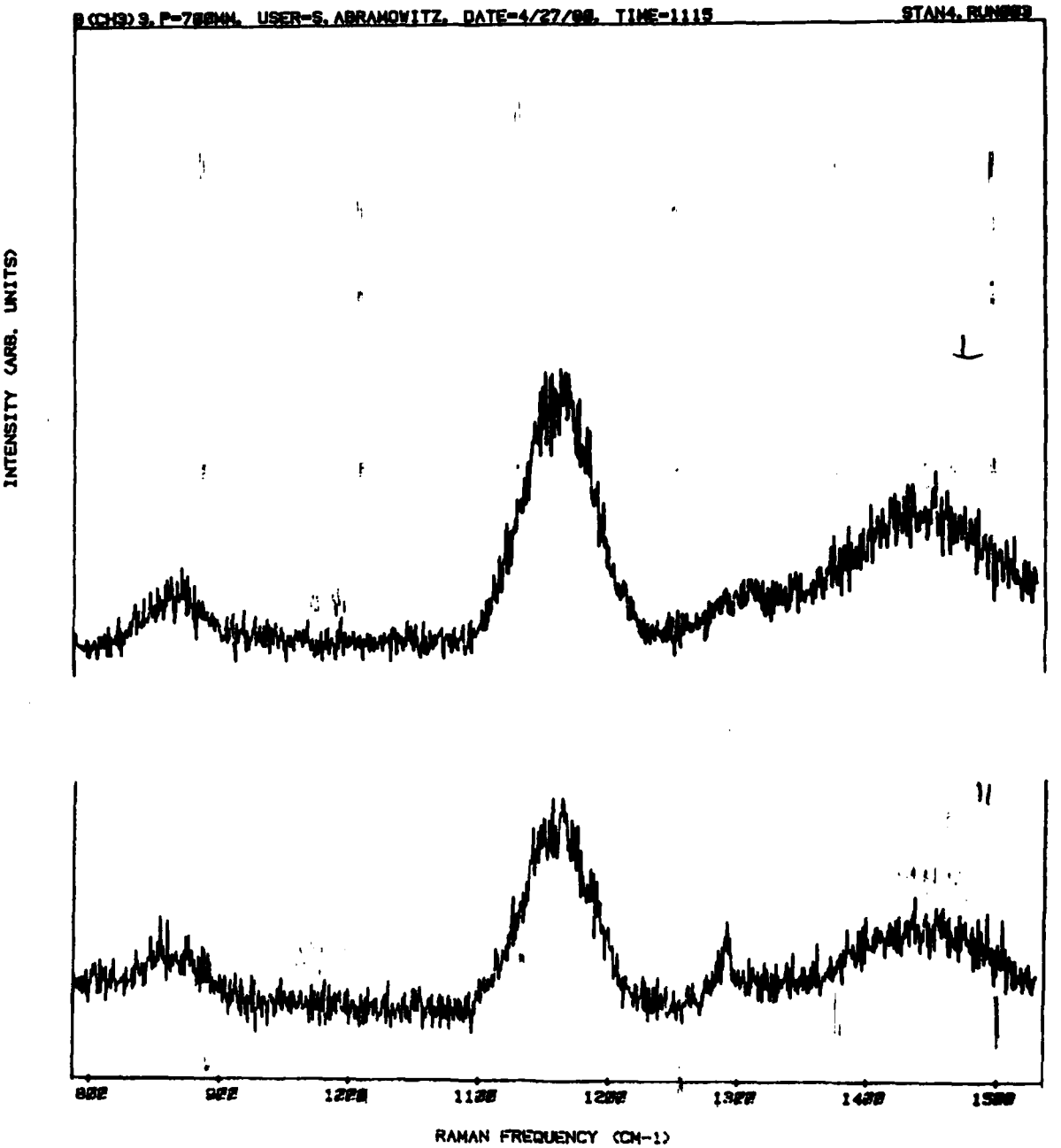
B(CH3)3, P=788MM, USER=S. ABRAHOWITZ, DATE=4/27/88, TIME=1115
STAN4, RUN#3
INTENSITY (ARB. UNITS)
800
900
1200
1100
1200
1300
1400
1500
RAMAN FREQUENCY (CM-1)

FIGURE 5

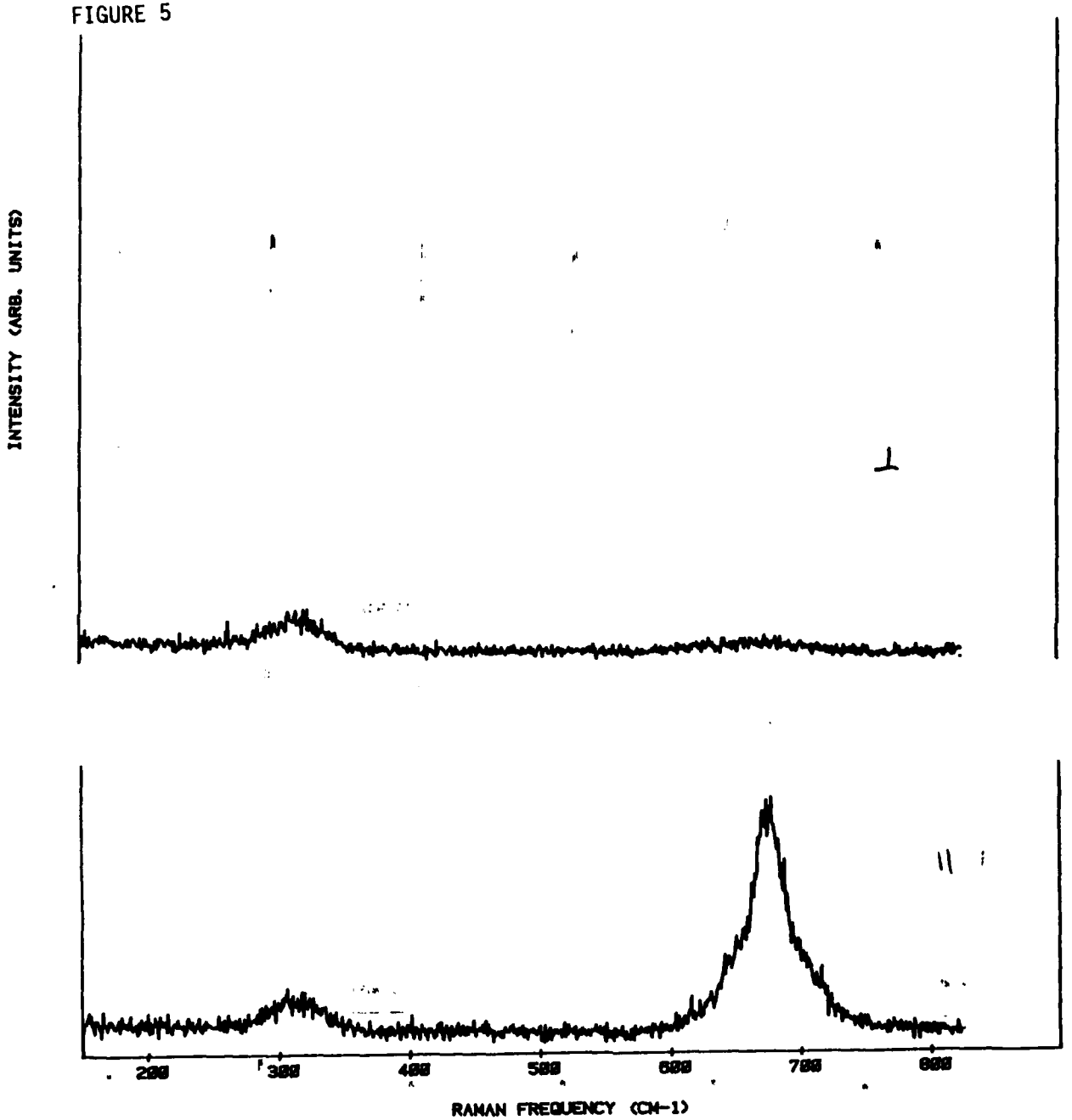
INTENSITY (ARB. UNITS)
200
300
400
500
600
700
800
RAMAN FREQUENCY (CM-1)

$B(CH_3)_3$

FIGURE 6 VAPOR PHASE SPECTRUM

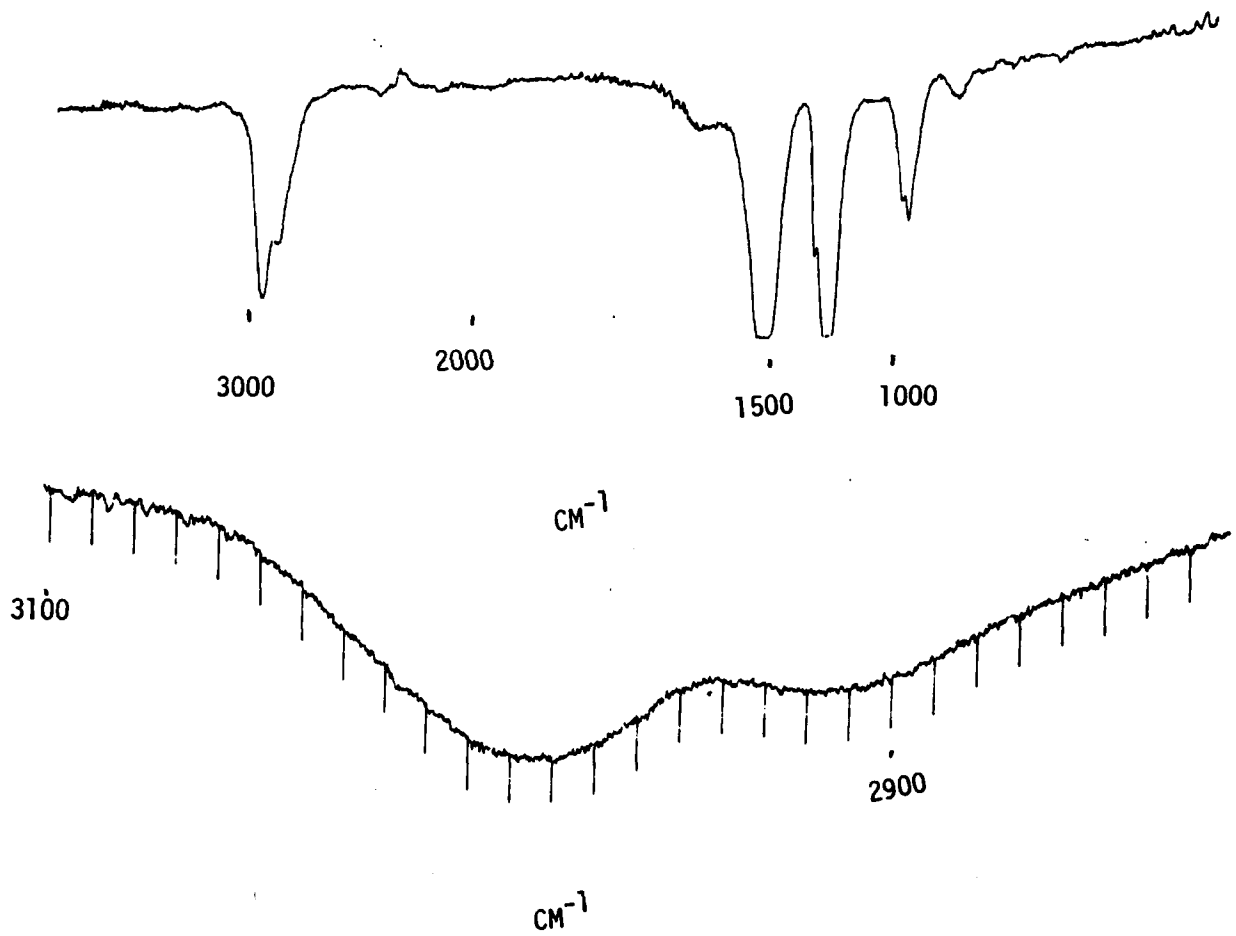

FIGURE 7 $B(CH_3)_3$ VAPOR PHASE SPECTRUM

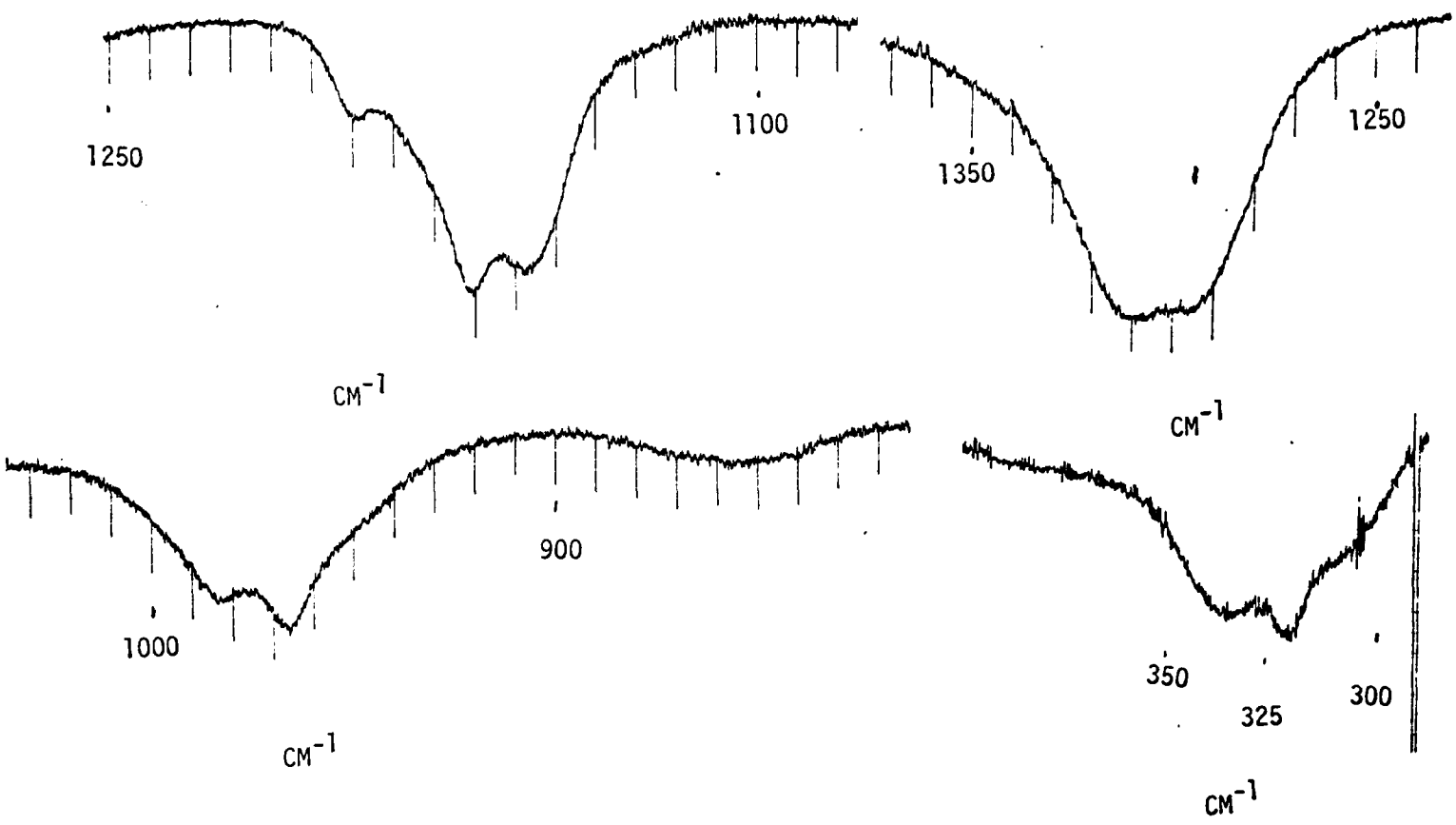


DAT
ILM